Collective Excitation of Rydberg-Atom Ensembles beyond the Superatom Model

Martin Gärttner,[1] Shannon Whitlock,[2] David W. Schönleber,[3,1] and Jörg Evers[1]
[1]*Max-Planck-Institut für Kernphysik, Saupfercheckweg 1, 69117 Heidelberg, Germany*
[2]*Physikalisches Institut, Universität Heidelberg, Im Neuenheimerfeld 226, 69120 Heidelberg, Germany*
[3]*Max-Planck-Institut für Physik komplexer Systeme, Nöthnitzer Straße 38, 01187 Dresden, Germany*
(Received 11 August 2014; published 2 December 2014)

In an ensemble of laser-driven atoms involving strongly interacting Rydberg states, the steady-state excitation probability is usually substantially suppressed. In contrast, here we identify a regime in which the Rydberg excited fraction is enhanced by the interaction. This effect is associated with the buildup of many-body coherences induced by coherent multiphoton excitations between collective states. The excitation enhancement should be observable under currently existing experimental conditions and may serve as a direct probe for the presence of coherent multiphoton dynamics involving collective quantum states.

DOI: 10.1103/PhysRevLett.113.233002 PACS numbers: 32.80.Ee, 32.80.Rm, 42.50.Nn

The emergence of collective quantum effects in a many-body system is a hallmark of the strongly correlated regime. A celebrated early example is the phenomenon of Dicke superradiance, in which N two-level atoms coherently interacting with a common optical field acquire enhanced emission properties [1]. In cavity quantum electrodynamics, an ensemble of N atoms placed inside an optical cavity experiences a collective enhancement of the coupling to a single cavity photon which scales as $\sqrt{N}$ [2,3]. Similar collective effects arise in the coupling of superconducting devices to nitrogen vacancy centers in diamond [4–6] and could play important roles in circuit QED [7] and hybrid optical-micromechanical systems [8]. Ensembles of highly excited Rydberg atoms offer an alternative system with which to study correlations and collective effects due to strong interatomic interactions. Here the competition between the laser excitation process and the interactions ensures only one Rydberg excitation can be accommodated within a critical distance (dipole blockade effect) leading to strong spatial correlations. In this regime, the atoms are excited to collective Dicke states, which leads to a $\sqrt{N}$ enhancement of the atom-light coupling [1,9]. In this spirit, one can describe the fully blockaded ensemble as a single "superatom" (SA) with a $\sqrt{N}$ larger transition dipole moment. This $\sqrt{N}$ enhancement of the atom-light coupling has been demonstrated [10–14]. By exploiting these effects, it should be possible to realize new quantum technologies such as nonclassical light sources [15–17] and quantum gates based on collectively enhanced interactions [9].

In this Letter, we point out an enhancement of the steady-state Rydberg population for driven three-level atoms which exceeds the predictions arising from the $\sqrt{N}$ enhancement typically associated with the dipole blockade effect. While the dipole blockade usually suppresses the fraction of Rydberg excited atoms as compared to the noninteracting case, the effect reported here instead enhances the Rydberg excited fraction. This enhancement occurs for a resonant two-step excitation from the ground state to the Rydberg state [under electromagnetically induced transparency (EIT) conditions] and for repulsive Rydberg-Rydberg interactions. We show that the effect is related to direct multiphoton transitions between collective states. As a result, its investigation requires calculations beyond simple superatom and rate-equation models. As this effect should be observable in existing cold atom experiments, it may serve as a direct probe for coherent multiphoton processes between collective states, as well as physics beyond the superatom and rate-equation pictures, via the measurement of a global steady-state observable.

First, we consider an ensemble of N three-level atoms all confined to a volume comparable to, or smaller than, a single blockade sphere [Fig. 1(a)]. The atoms are driven by two laser fields which couple the ground and intermediate state $|g\rangle \to |e\rangle$ and the intermediate and the Rydberg state $|e\rangle \to |r\rangle$ referred to as the probe and coupling transitions, respectively. The $|e\rangle$ state decays rapidly (decay rate Γ) via spontaneous emission to the ground state while the other two states are long-lived.

The Hamiltonian of this system reads ($\hbar = 1$)

$$H = \sum_{i=1}^{N} H_L^{(i)} - \sum_{i=1}^{N} \Delta \sigma_{ee}^{(i)} + \sum_{i<j} \frac{C_6 \sigma_{rr}^{(i)} \sigma_{rr}^{(j)}}{|\mathbf{x}_i - \mathbf{x}_j|^6}, \qquad (1)$$

where $H_L^{(i)} = \Omega_p/2\sigma_{ge}^{(i)} + \Omega_c/2\sigma_{er}^{(i)} + \text{H.c.}$ and $\mathbf{x}_i$ are the atomic positions. $\sigma_{ab}^{(i)} = |a_i\rangle\langle b_i|$ with $a, b \in \{e, g, r\}$ are operators acting on atom i, and we further define collective operators $\sigma_{ab} = \sum_i \sigma_{ab}^{(i)}$. We allow for a detuning Δ from the intermediate state as indicated in Fig. 1(a) and assume that the Rydberg states interact repulsively via isotropic van der Waals interactions with strength C_6. Incoherent processes like spontaneous emission and dephasing are treated using a master equation (ME) including Lindblad terms [18]. The resulting ME reads $\dot{\rho} = -i[H, \rho] + \mathcal{L}[\rho]$. We

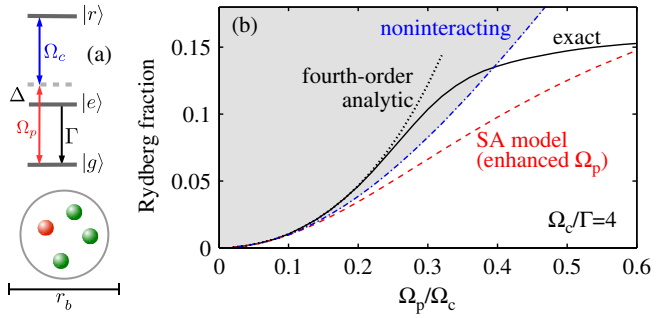

FIG. 1 (color online). (a) Illustration of the setup: Three-level atoms with the Rydberg state $|r\rangle$. The blockade radius exceeds the trap size such that at most one atom can be in the Rydberg state. (b) Steady-state values of the Rydberg fraction for $N = 4$ atoms as a function of the probe Rabi frequency ($\Delta = 0$). The coherent laser driving is strong compared to the decay rate Γ of the intermediate level. Solid black line: Rydberg fraction f_r predicted by the exact ME solution. Red dashed line: Result f_{SA} of a SA model with $\sqrt{N}$-enhanced Ω_p. Blue dot-dashed line: Rydberg fraction f_0 for noninteracting atoms. Black dotted line: Analytical expansion of f_r in the weak probe limit. The gray shading denotes the region of interaction-induced enhancement beyond the noninteracting value.

assume continuous spatially homogeneous laser driving and focus on the Rydberg fraction $f_r = N^{-1}\mathrm{Tr}[\sigma_{rr}\rho]$ in the steady state ($\dot{\rho} = 0$) as our main observable. We are able to simulate the dynamics and steady states for up to $N = 10$ three-level atoms using the wave function Monte Carlo method [19].

Solving the ME for a single atom ($N = 1$) and under perfect EIT conditions (zero dephasing and decay of the Rydberg state), up to a normalization factor, yields the steady state $|d\rangle = |g\rangle - \Omega_p/\Omega_c|r\rangle$, which is the EIT dark state. Thus, the Rydberg excitation probability, equivalent to the steady-state Rydberg fraction, becomes $f_0 = \Omega_p^2/(\Omega_c^2 + \Omega_p^2)$. In the case of a fully blockaded ensemble of $N > 1$ particles modeled as a SA, the resulting Rydberg excitation probability is obtained by replacing Ω_p with $\sqrt{N}\Omega_p$ in f_0, i.e., $Nf_{\mathrm{SA}} = N\Omega_p^2/(\Omega_c^2 + N\Omega_p^2)$. Comparing f_{SA} to f_0 shows that in the simple SA picture, the excitation probability cannot be enhanced more than N fold over the single-atom value, $Nf_{\mathrm{SA}} \leq Nf_0$. In the following, we will show that the Rydberg fraction f_r predicted by the exact solution of the ME can violate this bound. Thus, a collective excitation enhancement beyond the prediction of the SA model and even beyond the value f_0 of noninteracting atoms is possible.

This is illustrated in Fig. 1(b), which shows the Rydberg fraction f_r for a fully blockaded ensemble as a function of Ω_p/Ω_c for $N = 4$, $\Omega_c = 4\Gamma$, and $\Delta = 0$. Note that we operate in a regime where the total Rydberg fraction is small. Nevertheless, in the noninteracting case, the total Rydberg population includes a finite probability to excite two or more Rydberg atoms. Imposing perfect dipole blockade forces this component to vanish. For weak driving $\Omega_p \to 0$, the exact solution f_r agrees with the noninteracting (or single-atom) value f_0 as well as with f_{SA}. For large Ω_p, the Rydberg fraction approaches a constant value of $1/N$ due to the blockade, again consistent with the SA prediction. However, in between (for $0.15 \lesssim \Omega_p/\Omega_c \lesssim 0.4$), the Rydberg excited fraction $f_r > f_0$ significantly exceeds the noninteracting value. This feature is counter to the usual expectation for the dipole blockade in which repulsive interactions lead to a reduction of the number of Rydberg excitations compared to the noninteracting case. The red dashed line shows the prediction of the SA model, which predicts $f_{\mathrm{SA}} \leq f_0$, and is, thus, insufficient to explain the collective excitation enhancement.

To provide a physical picture for the excitation enhancement effect, we express the system in the basis of symmetrized Dicke states [1,9,20,21]. These states are fully symmetric superpositions of all excited states with the same number of e and r excitations,

$$|E^j R^s\rangle = \mathcal{N}_{j,s}(\sigma_{eg})^j(\sigma_{rg})^s|G\rangle \tag{2}$$

with the normalization $\mathcal{N}_{j,s}$ [18]. We use the shorthand notation $|E^0R^0\rangle = |G\rangle$, $|E^1R^0\rangle = |E\rangle$, and $|E^0R^1\rangle = |R\rangle$ [Fig. 2(a)]. Note that $s \in \{0, 1\}$ for a perfectly blockaded

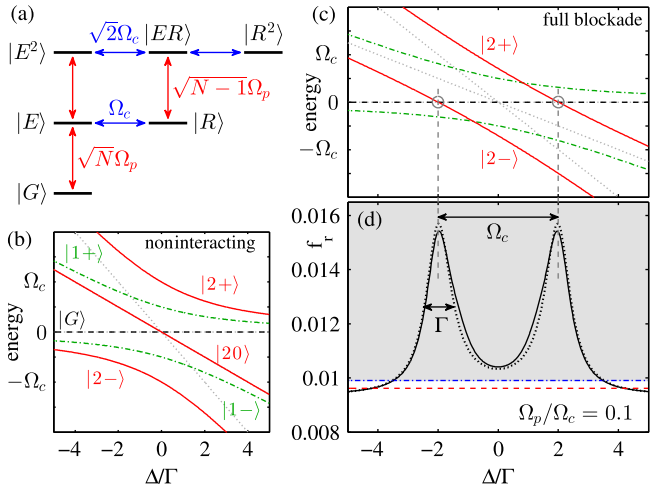

FIG. 2 (color online). (a) Level scheme of symmetrized (Dicke) states. Diagonalizing the horizontal couplings (Ω_c) in a perfectly blockaded ensemble, a dressed state picture is obtained. (b),(c) Dressed state energies as a function of the detuning from the intermediate state Δ in the (b) noninteracting and (c) blockaded cases. In the blockaded case resonances between the state $|G\rangle$ and the doubly excited dressed states (red) occur at $\Delta \approx \pm\Omega_c/2$ (circles). Gray dotted lines show bare energies (or asymptotes). (d) Rydberg fraction as a function of Δ. The parameters are as in Fig. 1. Solid black line: Exact ME solution. Red dashed line: Result of the SA model. Blue dot-dashed line: f_0. Black dotted line: Analytical model. The resonances between the dressed Dicke states result in a large excitation enhancement in comparison to the noninteracting Rydberg fraction.

ensemble, so the state $|R^2\rangle$ is not present in this case. The Hamiltonian (1) preserves the symmetry of these states, and population of states outside the manifold of symmetric states only arises due to incoherent effects such as spontaneous emission. The coupling laser does not change the total number of excitations $j+s$. Therefore, the Ω_c part of the Hamiltonian can be diagonalized, resulting in the dressed many-body eigenstates shown in Figs. 2(b) and 2(c). Because of the exclusion of states with multiple Rydberg excitations, the interacting system exhibits new level crossings. In particular, we point out the crossings between the states $|G\rangle$ and the dressed states of the $j+s=2$ manifold at $\Delta=\pm\Omega_c/2$. At these detunings, we expect an enhanced Rydberg excited fraction due to a direct transition involving two probe photons.

In the noninteracting case, a level crossing appears at $\Delta=0$; however, here the dressed Dicke state picture is incomplete since interference effects between different excitation channels are not visualized. Such effects lead to the absence of e excitations in the noninteracting case (EIT), and, thus, the noninteracting Rydberg fraction is independent of the intermediate state detuning Δ. Figure 2(d) shows the detuning dependence of the Rydberg fraction. The full calculations show a significant detuning dependence of f_r with two peaks centered around $\Delta\approx\pm\Omega_c/2$ with widths of $\approx\Gamma$. At its maximum, the enhancement is approximately a 50% effect. On resonance ($\Delta=0$), the enhancement is still visible, but only on the order of 5% for these parameters. Clearly, here the simple SA picture fails, since it amounts to neglecting all but the states $|G\rangle$, $|E\rangle$, and $|R\rangle$. The presence of the resonances, however, shows that states with $j+s>1$ play a crucial role. In particular, from the dressed state representation we find that coherent two-photon excitation from the ground to the doubly excited collective states is essential for the observed enhancement effect.

On resonance, this effect appears most surprising, as in the noninteracting case the dressed Dicke states show a crossing at $\Delta=0$, while in the blockaded case they do not. Therefore, in the following we focus on the excitation enhancement for the special case of $\Delta=0$. Figure 3(a) shows the ratio f_r/f_0 obtained from exact ME calculations as a function of the Rabi frequencies for the case of four fully blockaded atoms and perfect EIT conditions. For strong coupling and weak probe fields, we observe a range of parameters where the Rydberg fraction exceeds that of a noninteracting ensemble, $f_r>f_0$. The dashed line marks the border of this region ($f_r=f_0$). As N is increased, the qualitative features of this dissipative phase diagram stay the same and the structure is compressed vertically, consistent with a $\sqrt{N}$ rescaling of Ω_p, while the onset in Ω_c/Γ is independent of N in the weak probe limit. We also determine the values of Ω_p for which f_r/f_0 is maximized. For $\Omega_c=4\Gamma$, the maximum is found at $\sqrt{N}\Omega_p\approx 0.5\Omega_c$. Figure 3(b) shows the maximal value of f_r/f_0 as a function

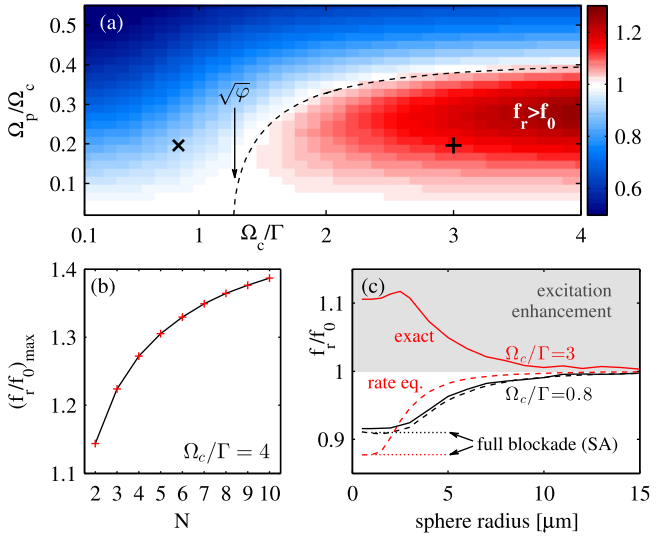

FIG. 3 (color online). (a) Dissipative phase diagram showing the enhancement factor f_r/f_0 as a function of Rabi frequencies for $N=4$ atoms and $\Delta=0$. For strong coherent driving and weak probe field, a region of $f_r>f_0$ is encountered. The dashed line shows the transition from suppressed to enhanced excitation ($f_r=f_0$). The arrow marks the critical value of $\Omega_c/\Gamma\approx 1.27$. (b) Maximal value of f_r/f_0 as a function of atom number N. (c) Few atoms ($N=4$) in a spherical volume of varying radius with random position sampling. The possibility for multiple Rydberg excitations is included in the simulation, and realistic values for the laser dephasings and the spontaneous decay rate of the Rydberg state have been used (see text for details). The parameters correspond to the black cross (lower black curves) and plus sign (upper red curves) in (a). For the higher Rabi frequencies, the excitation enhancement is present at all sphere radii (densities). Dashed lines show the predictions of the rate equation model, which coincide with the SA model in the case of full blockade (dotted lines).

of the atom number N. We find that f_r/f_0 appears to saturate but reaches values larger than 1.4 if extrapolated to larger N. Similarly, the enhancement factor saturates as a function of Ω_c/Γ.

In the following, we derive analytical expressions for the Rydberg fraction for a fully blockaded ensemble using fourth-order perturbation theory for small Ω_p/Ω_c. By dividing the ME by $\Omega_c/2$, we separate off the term associated with probe laser proportional to $\epsilon=\Omega_p/\Omega_c$, which can be treated as a perturbation in the weak probe limit. We then expand the steady-state density matrix in orders of the small parameter ϵ ($\rho=\sum_n\rho_n\epsilon^n$) and solve for the ρ_n recursively [18]. To fourth order, we obtain $f_r^{(4)}=\epsilon^2+c_4\epsilon^4+\mathcal{O}(\epsilon^6)$ where

$$c_4=2(N-1)\frac{1+4\mathrm{Im}[\beta]^2-|\beta|^2-|\beta|^4}{|1+\beta^2|^2}-1 \qquad (3)$$

with $\beta=(\Gamma+2i\Delta)/\Omega_c$. The predictions of Eq. (3) are shown as dotted lines in Figs. 1(b) and 2(d). We can now

compare the fourth-order terms in the noninteracting case $f_0=\epsilon^2-\epsilon^4+\mathcal{O}(\epsilon^6)$, the SA case $f_{\mathrm{SA}}=\epsilon^2-N\epsilon^4+\mathcal{O}(\epsilon^6)$, and the master equation calculation $f_r^{(4)}$. By solving $c_4>-1$ for β with $\Delta=0$, we find that enhancement ($f_r>f_0$) occurs if $\Omega_c/\Gamma>\sqrt{\varphi}$ with $\varphi=(\sqrt{5}-1)/2$, independent of N [arrow in Fig. 3(a)]. A closer analysis of c_4 reveals that in the limit $\Omega_c\gg\Gamma$, Eq. (3) describes two Lorentzian peaks of width Γ centered at $\Delta=\pm\Omega_c/2$. The enhancement of the fourth-order term beyond the noninteracting value is $c_4+1\approx 2(N-1)$ on resonance ($\Delta=0$), while at the maxima ($\Delta=\pm\Omega_c/2$) one obtains $c_4+1\approx 3\Omega_c^2(N-1)/(2\Gamma^2)$.

We now ask if the enhancement effect persists under realistic experimental conditions, for example, with imperfect blockade and including dephasing and the finite lifetime of the Rydberg state. We consider ^{87}Rb atoms with states $|g\rangle=|5s_{1/2}\rangle$, $|e\rangle=|5p_{3/2}\rangle$, and $|r\rangle=|55s\rangle$ as in Ref. [22]. The atoms are assumed to be randomly distributed inside a sphere of variable radius. The corresponding interaction coefficient is $C_6/2\pi=50\ \mathrm{GHz}\,\mu\mathrm{m}^6$, and the spontaneous decay rates are $\Gamma/2\pi=6.06$ MHz and $\Gamma_r/2\pi=2$ kHz. An overview of the simulations is shown in Fig. 3(c) (solid lines). The lower black lines correspond to the Rabi frequencies $\Omega_p/2\pi=1$ MHz, $\Omega_c/2\pi=5.1$ MHz, and the laser linewidths $\gamma_p/2\pi=0.33$ MHz and $\gamma_c/2\pi=1.4$ MHz, typical of recent experiments [22]. The upper red lines correspond to the strong driving case with both Rabi frequencies increased by a factor of 3.75. In the case of weak driving, no excitation enhancement is observed. For strong driving, f_r/f_0 exceeds unity and increases towards higher densities (smaller sphere radii). Although the laser dephasings are chosen relatively large, the enhancement persists for all densities. This means that collective excitation enhancement should be observable under realistic experimental conditions as long as the regime of strong coherent driving ($\Omega_c/\Gamma>\sqrt{\varphi}$) is reached. Through time-dependent simulations, we also verified that the steady state is reached in less than 1 μs for these parameters. One option to observe the excitation enhancement could, thus, be to vary the cloud density at a constant atom number, for example, by thermal expansion.

The observation of the collective enhancement has important consequences for understanding light-matter interactions in strongly interacting systems. Our results indicate that the coherences between N-atom collective states and direct two-photon processes crucially influence the steady state of the system. Classical rate-equation models [22–28] which neglect these coherences are not sufficient in this regime. While these models do reproduce the physics associated to the usual $\sqrt{N}$ enhancement, they cannot describe the enhancement effect reported here since $f_r<f_0$ is assumed by construction [28]. To illustrate this, the predictions of a rate-equation model [26] have been added as dashed lines in Fig. 3(c).

The excitation enhancement, therefore, acts as a clear experimental signature for the breakdown of the rate-equation approach, indicating a regime in which qualitatively new results can be expected. As an example, we consider the nonlinear optical response of a Rydberg gas driven under EIT conditions, which is predicted to obey a universal relation between the nonlinear absorption coefficient $\chi=\mathrm{Im}[\chi_{eg}]$ and the Rydberg fraction f_r [23,25,28]. The range of validity covered by this relation is linked to that of the rate-equation model [28]. The universal relation states that in the case of perfect EIT, $\chi/\chi_{2L}=1-f_r/f_0$. Here, $\chi_{eg}\propto N^{-1}\langle\sigma_{ge}\rangle$ is the probe field susceptibility (see Ref. [23] for details), and χ_{2L} is the corresponding two-level absorption, i.e., without the coupling laser. However, $f_r>f_0$ would imply a negative susceptibility, which is impossible as the optical Bloch equations predict $\chi\propto\langle\sigma_{ee}\rangle>0$. Hence, the universal relation must break down under conditions in which collective excitation enhancement occurs.

Additionally, the enhancement effect sheds light on the role of decoherence. Typically, it is challenging to distinguish between coherent and incoherent excitation dynamics [29–38]. However, the effect observed here manifests itself in a global observable in steady state and is, thus, comparatively easy to access experimentally. Since the enhancement is associated with a direct two-photon process, it requires at least partly coherent dynamics. Indeed, we find that if single-atom dephasing is added, f_r/f_0 decreases monotonically and falls below unity when dephasing dominates.

In summary, we have discovered a counterintuitive collective excitation enhancement effect that occurs for strong driving of the upper and weak driving of the lower transition of interacting three-level Rydberg atoms. We have shown that this effect is connected to direct multiphoton transitions between collective Dicke states and have derived analytical expressions for the steady-state density for arbitrary atom number N, which are capable of reproducing the observed enhancement effect in the weak probe limit. The enhancement allows us to detect the presence of coherent multiphoton processes and to identify parameter regimes in which the rate equation approach breaks down. As the enhancement involves a global steady-state observable, it should be observable with existing experimental setups [16,17,22,35].

A natural next step would be to ask how the observed excitation enhancement is connected to the buildup of multipartite entanglement. Furthermore, it is interesting to ask whether similar enhancements could be observed in other strongly interacting driven systems, or if the generated multiparticle coherences will find applications in metrology or in quantum information science.

We thank K. P. Heeg and M. Höning for discussions. This work was supported by University of

Heidelberg (Center for Quantum Dynamics, Landesgraduiertenförderung). S. W. acknowledges support by the Deutsche Forschungsgemeinschaft Emmy Noether Grant No. Wh141-1-1.

[1] R. H. Dicke, Phys. Rev. **93**, 99 (1954).
[2] Y. Colombe, T. Steinmetz, G. Dubois, F. Linke, D. Hunger, and J. Reichel, Nature (London) **450**, 272 (2007).
[3] F. Brennecke, T. Donner, S. Ritter, T. Bourdel, M. Kohl, and T. Esslinger, Nature (London) **450**, 268 (2007).
[4] Y. Kubo, F. R. Ong, P. Bertet, D. Vion, V. Jacques, D. Zheng, A. Dréau, J.-F. Roch, A. Auffeves, F. Jelezko, J. Wrachtrup, M. F. Barthe, P. Bergonzo, and D. Esteve, Phys. Rev. Lett. **105**, 140502 (2010).
[5] X. Zhu, S. Saito, A. Kemp, K. Kakuyanagi, S.-i. Karimoto, H. Nakano, W. J. Munro, Y. Tokura, M. S. Everitt, K. Nemoto, M. Kasu, N. Mizuochi, and K. Semba, Nature (London) **478**, 221 (2011).
[6] R. Amsüss, C. Koller, T. Nöbauer, S. Putz, S. Rotter, K. Sandner, S. Schneider, M. Schramböck, G. Steinhauser, H. Ritsch, J. Schmiedmayer, and J. Majer, Phys. Rev. Lett. **107**, 060502 (2011).
[7] A. Wallraff, D. I. Schuster, A. Blais, L. Frunzio, R.-S. Huang, J. Majer, S. Kumar, S. M. Girvin, and R. J. Schoelkopf, Nature (London) **431**, 162 (2004).
[8] B. Vogell, K. Stannigel, P. Zoller, K. Hammerer, M. T. Rakher, M. Korppi, A. Jöckel, and P. Treutlein, Phys. Rev. A **87**, 023816 (2013).
[9] M. D. Lukin, M. Fleischhauer, R. Côté, L. M. Duan, D. Jaksch, J. I. Cirac, and P. Zoller, Phys. Rev. Lett. **87**, 037901 (2001).
[10] R. Heidemann, U. Raitzsch, V. Bendkowsky, B. Butscher, R. Löw, L. Santos, and T. Pfau, Phys. Rev. Lett. **99**, 163601 (2007).
[11] A. Gaëtan, Y. Miroshnychenko, T. Wilk, A. Chotia, M. Viteau, D. Comparat, P. Pillet, A. Browaeys, and P. Grangier, Nat. Phys. **5**, 115 (2009).
[12] E. Urban, T. A. Johnson, T. Henage, L. Isenhower, D. D. Yavuz, T. G. Walker, and M. Saffman, Nat. Phys. **5**, 110 (2009).
[13] Y. O. Dudin, L. Li, F. Bariani, and A. Kuzmich, Nat. Phys. **8**, 790 (2012).
[14] D. Barredo, S. Ravets, H. Labuhn, L. Béguin, A. Vernier, F. Nogrette, T. Lahaye, and A. Browaeys, Phys. Rev. Lett. **112**, 183002 (2014).
[15] Y. O. Dudin and A. Kuzmich, Science **336**, 887 (2012).
[16] T. Peyronel, O. Firstenberg, Q.-Y. Liang, S. Hofferberth, A. V. Gorshkov, T. Pohl, M. D. Lukin, and V. Vuletic, Nature (London) **488**, 57 (2012).
[17] D. Maxwell, D. J. Szwer, D. Paredes-Barato, H. Busche, J. D. Pritchard, A. Gauguet, K. J. Weatherill, M. P. A. Jones, and C. S. Adams, Phys. Rev. Lett. **110**, 103001 (2013).
[18] See Supplemetal Material at http://link.aps.org/supplemental/10.1103/PhysRevLett.113.233002 for details on the master equation, the symmetrized Dicke basis, and the analytical calculation of the steady state.
[19] K. Mølmer, Y. Castin,, and J. Dalibard, J. Opt. Soc. Am. B **10**, 524 (1993).
[20] A. Carmele, B. Vogell, K. Stannigel, and P. Zoller, New J. Phys. **16**, 063042 (2014).
[21] Y.-M. Liu, D. Yan, X.-D. Tian, C.-L. Cui, and J.-H. Wu, Phys. Rev. A **89**, 033839 (2014).
[22] C. S. Hofmann, G. Günter, H. Schempp, M. Robert-de-Saint-Vincent, M. Gärttner, J. Evers, S. Whitlock, and M. Weidemüller, Phys. Rev. Lett. **110**, 203601 (2013).
[23] C. Ates, S. Sevinçli, and T. Pohl, Phys. Rev. A **83**, 041802 (2011).
[24] D. Petrosyan, J. Otterbach, and M. Fleischhauer, Phys. Rev. Lett. **107**, 213601 (2011).
[25] S. Sevinçli, C. Ates, T. Pohl, H. Schempp, C. S. Hofmann, G. Günter, T. Amthor, M. Weidemüller, J. D. Pritchard, D. Maxwell, A. Gauguet, K. J. Weatherill, M. P. A. Jones, and C. S. Adams, J. Phys. B **44**, 184018 (2011).
[26] K. P. Heeg, M. Gärttner, and J. Evers, Phys. Rev. A **86**, 063421 (2012).
[27] M. Gärttner and J. Evers, Phys. Rev. A **88**, 033417 (2013).
[28] M. Gärttner, S. Whitlock, D. W. Schönleber, and J. Evers, Phys. Rev. A **89**, 063407 (2014).
[29] T. E. Lee, H. Häffner, and M. C. Cross, Phys. Rev. Lett. **108**, 023602 (2012).
[30] T. E. Lee and M. C. Cross, Phys. Rev. A **85**, 063822 (2012).
[31] H. Schempp, G. Günter, M. Robert-de-Saint-Vincent, C. S. Hofmann, D. Breyel, A. Komnik, D. W. Schönleber, M. Gärttner, J. Evers, S. Whitlock, and M. Weidemüller, Phys. Rev. Lett. **112**, 013002 (2014).
[32] D. W. Schönleber, M. Gärttner, and J. Evers, Phys. Rev. A **89**, 033421 (2014).
[33] N. Malossi, M. M. Valado, S. Scotto, P. Huillery, P. Pillet, D. Ciampini, E. Arimondo, and O. Morsch, Phys. Rev. Lett. **113**, 023006 (2014).
[34] T. M. Weber, M. Höning, T. Niederprüm, T. Manthey, O. Thomas, V. Guarrera, M. Fleischhauer, G. Barontini, and H. Ott, arXiv:1407.3611.
[35] P. Schauß, M. Cheneau, M. Endres, T. Fukuhara, S. Hild, A. Omran, T. Pohl, C. Gross, S. Kuhr, and I. Bloch, Nature (London) **491**, 87 (2012).
[36] D. Petrosyan, J. Phys. B **46**, 141001 (2013).
[37] I. Lesanovsky and J. P. Garrahan, Phys. Rev. A **90**, 011603 (2014).
[38] A. Urvoy, F. Ripka, I. Lesanovsky, D. Booth, J. Shaffer, T. Pfau, and R. Löw, arXiv:1408.0039.